DOI: 10.2352/ISSN.2470-1173.2016.14.IPMVA-372
Reprinted from
Journal of Imaging Science and Technology® 59(6): 060403-1–060403-11, 2015.

Development of a Multi-Resolution Microscopy Image Processing System

Tomohiro Suzuki
Graduate School of Engineering, Shizuoka University, 3-5-1 Johoku, Nakaku, Hamamatsu, Shizuoka, Japan
E-mail: suzuki.tomohiro.14@shizuoka.ac.jp

Shin Usuki
Research Institute of Electronics, Shizuoka University, 3-5-1 Johoku, Nakaku, Hamamatsu, Shizuoka, Japan

Kenjiro T. Miura
Graduate School of Engineering, Shizuoka University, 3-5-1 Johoku, Nakaku, Hamamatsu, Shizuoka, Japan

Abstract. *With the miniaturization of precision machine components, the measurement of data at a high resolution is important for product inspection. Microscopy measurement techniques have been improved to a high resolution so as to satisfy the need. However, since the range of high-resolution measurement is narrow, it is difficult to observe the entire structure of the target at a time. If it is possible to unify many measurement data taken under different conditions into one dataset while keeping the positional relationships between the data, one can effectively observe details and understand the entire structure. Hence, we develop an image processing system that synthesizes measurement data with different resolutions and displays both the entire structure and fine details of the observed object simultaneously. In order to unify the measurement data, we propose two image synthesis methods based on feature points and edge information. This article also describes the details of the system which can generate multi-resolution models by using the proposed methods and allows users to arbitrarily vary the display area and magnification while observing the entire structure.* © *2015 Society for Imaging Science and Technology.*
[DOI: 10.2352/J.ImagingSci.Technol.2015.59.6.060403]

INTRODUCTION

In recent years, the miniaturization of precision machine components has meant that measurement data with high resolution have been required for product inspection. There have been rapid developments in measurement techniques using microscopes at the nano- and micro-scale. However, microscopes cannot obtain much information because the depth of field and shooting range of a microscope are much less than those of a camera. Therefore, various microscopes need to be used, and the magnification needs to be adjusted according to the situation. Furthermore, it is important for product inspection that the positional relationship of each image be understood. One method creates and views high-resolution gigapixel images by capturing and coupling images.[1] However, coupling and showing all data with a high resolution at the nano-/micro-scale considerably increases the amount of memory required and the image size. Moreover, it is difficult to synthesize microscopy images taken under different conditions into one image and display them while preserving each pixel.

For these reasons, the measurement data cannot be effectively used. Hence, little research has gone into geometric modeling at the nano-/micro-scale. It is difficult to process data with different resolutions, synthesize a large amount of measurement data, and detect 3D shapes at high speeds. In order to solve these problems, we employ for microscopy measurement and image processing the idea of multi-resolution, which is well studied in the computer graphics (CG) field.[2] In microscopy measurement, the image resolution is very important. We develop a system that can display images while maintaining the pixel resolution by using multi-resolution techniques. As far as we know, there is no prior research that uses multi-resolution in the measurement and image processing fields at the nano-/micro-scale, and our study takes a quite new approach.

In this article, we propose a system that can effectively use measurement data taken under different conditions and simultaneously display the entire structure and local geometric properties of the observed object. In the second section, we describe the outline of our system. In the third and fourth sections, we synthesize measurement data taken under different conditions into one dataset by image processing. Next, we develop a system so that users can arbitrarily operate and obtain the entire structure and fine details of the observed object. In the fifth section, we describe the multi-resolution model and the result of applying our system to measurement data. By using this system, the user can obtain the necessary information while understanding the positional relationships between each image. This system is low cost while providing a high throughput and low memory consumption.

OUTLINE OF THE MULTI-RESOLUTION MICROSCOPY IMAGE PROCESSING SYSTEM

In a microscopy image, the display method of the observed object changes depending on the shooting conditions. It is

Received June 29, 2015; accepted for publication Sept. 21, 2015; published online Nov. 20, 2015. Associate Editor: Henry Y. T. Ngan.
1062-3701/2015/59(6)/060403/11/$25.00

DOI: 10.2352/ISSN.2470-1173.2016.14.IPMVA-372

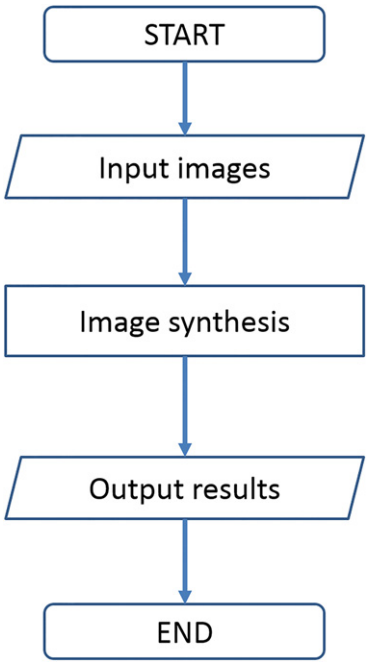

Figure 1. Flowchart of the synthesis module.

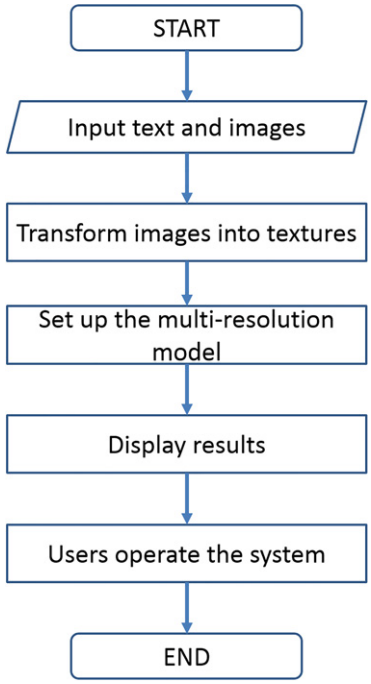

Figure 2. Flowchart of the view module.

difficult to display images shot under different conditions at the same time, so the user barely understands the positional relationships between each image. In our study, we matched the display magnification of different images to develop a multi-resolution model. In the model, these images are coupled, and high-resolution images are displayed on low-resolution images. We developed a system for users to see a selected range.

Our system comprises two modules: a synthesis module and a view module. The synthesis module collects the necessary information by inputting images to generate the multi-resolution model. The view module reads the information and generates the multi-resolution model. Figures 1 and 2 show the flowcharts of each module.

First, the synthesis module reads selected images. This module has two image synthesis methods based on feature points and edge information. One of the methods is selected depending on the images. The feature point method uses the speeded-up robust features (SURF) method[2] in an area selected by the user. This module couples input images with a feature point and calculates the necessary information to generate the multi-resolution model. Then, it generates a synthesized image and text file with the necessary information. When using the edge information method, the synthesis module converts input images into edge images and detects geometric configurations of images with random sample consensus (RANSAC). Then, the module couples input images with geometric configurations and calculates the necessary information to generate the multi-resolution model. Our system does not use the shooting conditions to calculate information, such as the image magnification and the use of microscopes.

The view module generates and displays the multi-resolution model. First, this module reads images and information from the text file output by the synthesis module. Next, it converts input images into textures and adjusts the difference between each texture size. All images are subjected to this process. The multi-resolution model is generated by arranging the textures appropriately. Two windows are created which display the entire image and a detailed image. Thus, the multi-resolution model can be operated by the user to arbitrarily operate the display magnification and obtain the entire structure and fine details of the observed object.

IMAGE SYNTHESIS METHOD BASED ON FEATURE POINT

We needed to unify the display magnifications and angles to display images under different conditions in parallel. Our system uses two image synthesis methods. In this section, we discuss the method based on feature detection.

Feature Detection with SURF

SURF is a feature point detection algorithm. The SURF process involves key point detection and feature quantity extraction. SURF detects robust features for scale transition and rotation. The advantages of SURF are its robustness against noise and short computation time compared with scale-invariant feature transform (SIFT).[3] We used these advantages to match images by using SURF. However, SURF cannot utilize image features obtained from the color space since SURF is processed in the gray space. We only use data measured with an optical microscope currently. Nevertheless, our target is not only optical microscopy images but also other microscopy images. For example, since measurement images obtained with a scanning electron microscope are gray scale, we cannot apply a method that uses the color information of these images. Thus, we use

DOI: 10.2352/ISSN.2470-1173.2016.14.IPMVA-372

SURF in this article. For future research, color information is very useful when the target data relate to a color image. Hence, that can be a subject of future study. In our system, the user selects the region of interest in order to couple images precisely. However, data that are matched with this method are not always correct. We can remove errors from the corresponding data by using RANSAC.[4] When there are n data, $(x_1, x_2), \ldots, (x_n, y_n)$, RANSAC randomly selects several data from all data and calculates parameters under the calculation conditions. Next, this method evaluates the validity of the parameters with other data. After repeating this process for a predetermined number of times, it extracts parameters with maximum evaluation and data supporting these parameters. At this time, errors are removed. Finally, we get conclusive parameters by applying a least square method to the extraction data. In our system, we improve the precision of matching by using RANSAC.

Unify Display Magnifications and Angles

Our method detects two feature points with a high similarity in two input images to unify the different magnifications by using SURF. The feature quantity of SURF is structured to contain 64 or 128 component vectors per point. In order to detect a corresponding feature point in two images, the difference in the feature quantity D is defined as

$$D = \sqrt{\sum_{i=1}^{128} (a_i - b_i)^2}, \tag{1}$$

where a and b are feature quantities of images A and B and i is a component of a feature vector. Eq. (1) is applied to all combinations of feature points. The combination with the lowest D is the most similar and represents matching points. In order to detect two combinations with the highest similarity, the distance between feature points d is given by the L2 norm and is defined as

$$d = \sqrt{(x_a - x_b)^2 + (y_a - y_b)^2}. \tag{2}$$

When the magnification of image A is equal to that of image B, the distance between image A's feature points d_a is equal to the distance between image B's feature points d_b. Thus, the magnification ratio R is defined as

$$R = \frac{d_a}{d_b}. \tag{3}$$

The image magnifications can be unified by multiplying R by the size of image B. The threshold is set based on the area selected by the user and the size of the input image. When R has no threshold, the system regards the result as a failure. In this case, the resolution can be decreased by down-sampling the high-resolution image. The feature points are then detected again while the resolution of the high-resolution image is lowered to be closer to that of the low-resolution image.

Next, images are rotated to unify their tilts. We can assume that feature points A and B of the low-resolution image correspond to feature points A' and B' of the high-resolution image. Given that the high-resolution image is inclined at an angle of θ degrees and that the coordinates of A are located at the coordinates of B, the angle between lines AB and $A'B'$ is also θ. Thus, θ is defined as

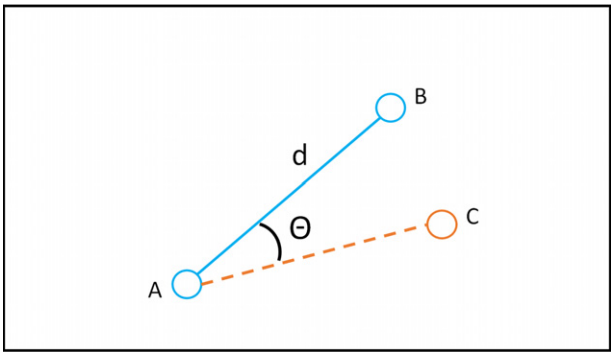

Figure 3. Schematic of the positional relationship of points.

$$\theta = \arctan\frac{y_b - y_a}{x_b - x_a} - \arctan\frac{y_{b'} - y_a}{x_{b'} - x_a}, \tag{4}$$

where x_a and y_a are the coordinates of A, x_b and y_b are the coordinates of B, and $x_{a'}$ and $y_{a'}$ are the coordinates of A'. The tilt between images can be matched by rotating the high-resolution image by θ. Figure 3 shows a schematic. The coordinates before rotation are defined as (x_i, y_i), the coordinates after rotation are defined as (x_j, y_j), and the coordinates of the center of rotation are defined as (x_r, y_r). Then, (x_r, y_r) can be defined as

$$x_i = \cos\theta(x_i - x_r) - \sin\theta(y_i - y_r) + x_r, \tag{5}$$

$$y_i = \sin\theta(x_i - x_r) + \cos\theta(y_i - y_r) + y_r. \tag{6}$$

The display angle can be unified by arranging the images at the coordinates calculated with Eqs. (5) and (6).

Brightness Adjustment of Images

If images taken under different conditions are displayed together, the brightness will differ at each spot. Thus, the brightness in all images needs to be adjusted for better display. One border processing method for image processing is Poisson image editing.[5] This method varies pixel values while keeping the edges of the original image—that is, it can adjust pixel values with the remaining image feature. However, it also changes information other than the brightness. This method is not suitable for our system because information needs to be kept for product inspection. For this reason, our system adjusts the pixel value directly to only change the brightness. For the hue saturation value (HSV), only the brightness is adjusted so that other information is kept. The brightness is defined by

$$B_d = B_{ave1} - B_{ave2}, \tag{7}$$

$$I' = I + B_d, \tag{8}$$

where B_{ave1} and B_{ave2} are average brightnesses of area in each image, B_d is the difference of average brightness, I

DOI: 10.2352/ISSN.2470-1173.2016.14.IPMVA-372

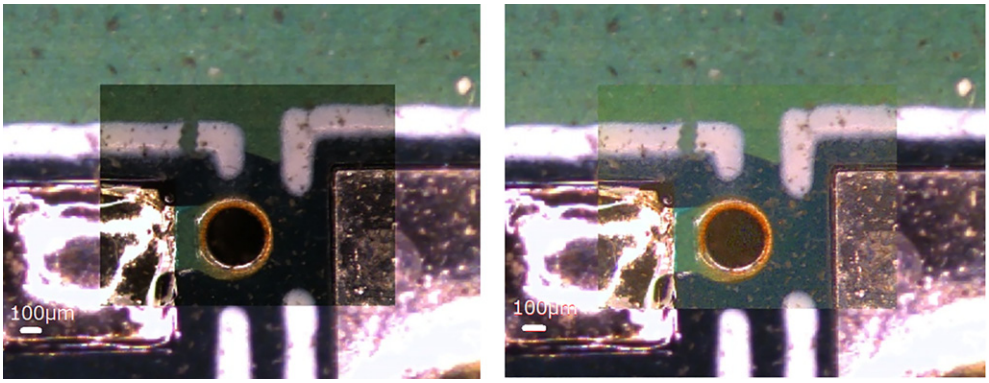

Figure 4. Result of brightness adjustment.

is a pixel value before brightness adjustment and I' is a pixel value after brightness adjustment. First, the difference between the average brightness of a high-resolution image and the average brightness of an area selected by the user in a low-resolution image is calculated. Next, the difference is added to all pixels of the high-resolution image. This brightens the high-resolution image and reduces the difference in brightness. Figure 4 shows the border area between high- and low-resolution images. The left image is the original, and the right image is the result after brightness adjustment. Fig. 4 shows that the difference in brightness is decreased by the adjustment. There are other differences and a border, but only the brightness is changed. The high-resolution image is not blurred, so its information is kept. In this instance, we applied the common method as the primary study. However, there are various algorithms.[6] Measurement data from microscopes have a lot of noise. In future work, we will study other brightness adjustment algorithms.

Result of Image Synthesis Based on Feature Point

Images captured with different magnifications can be synthesized by using the method presented in the previous sections. We took a picture of an electronic board. Table I lists the conditions. Figure 5 shows the base image with the lowest magnification, Figure 6 shows the image with the highest magnification, and Figure 7 shows the image synthesis result. We used five images that were captured with different magnifications from 0.75 to 6. As a result, we were able to synthesize images with different magnifications. The processing time was 1.342 s. The CPU and the main memory of the PC used for the experiment were Intel Core i7-870 and 8.00 GB.

Table I. Shooting conditions with an optical microscope.

Objective	Nikon ED Plan 1 × NA0.09
Zoom lens	0.75–7.5 power
Camera	1/2″ C-MOS digital camera
Sensor resolution	2048 × 1536 pixels
Light source	Halogen ring light

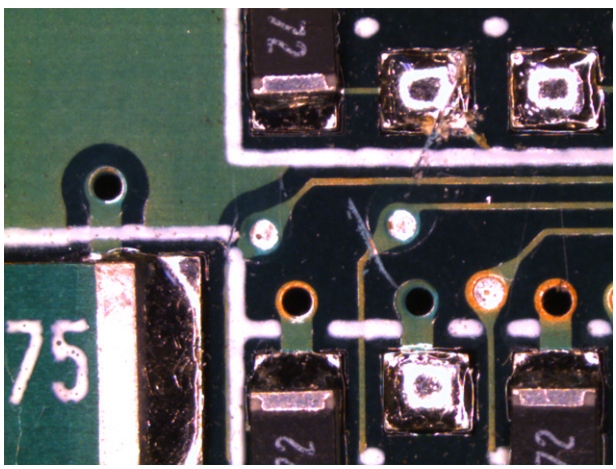

Figure 5. Image with lowest magnification.

IMAGE SYNTHESIS METHOD BASED ON EDGE INFORMATION

Outline of the Method Based on Edge Information

The method based on feature points can be used to synthesize data measured with an optical microscope at different magnifications. However, if a picture is taken of the same target under different conditions (e.g., different microscope or sensor), the feature points and quantities vary. It is difficult to synthesize images that are captured under different conditions by using the method based on feature points because SURF detects local features based on the brightness gradient around a target pixel. Hence, we propose a new method based on edge information.

This method converts input images into edge images. Lines are extracted from the edge images, and their equations are calculated. Then, images are matched by using points of intersection between these lines. Finally, two images are synthesized by applying affine transformation to matching points.

DOI: 10.2352/ISSN.2470-1173.2016.14.IPMVA-372

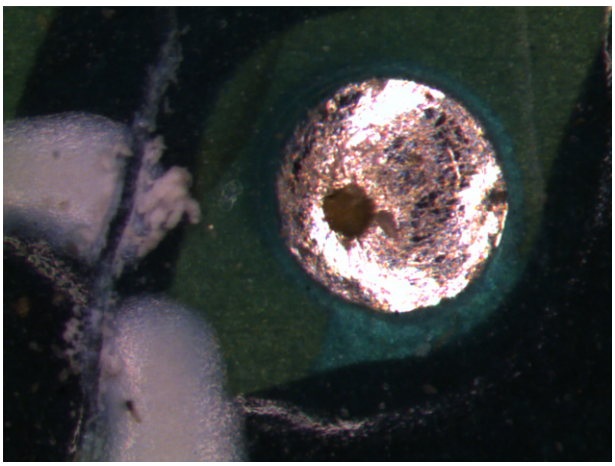

Figure 6. Image with highest magnification.

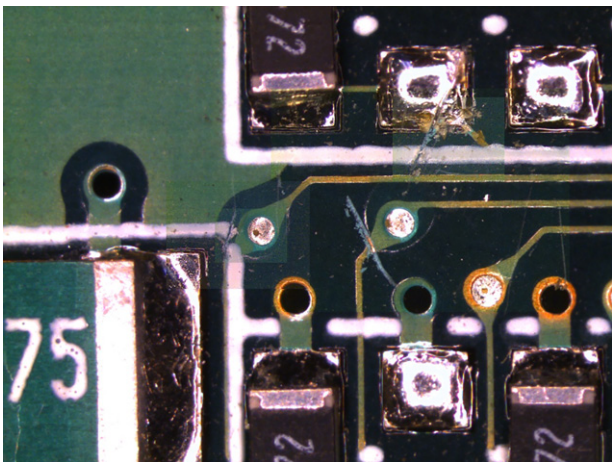

Figure 7. Result of image synthesis based on feature point.

Edge Detection for Microscopy Images

In our method, measured images are converted into edge images with an edge extraction method based on the separability of image features.[7,8] In this method, an edge is defined not as a point where the intensity changes rapidly but as a boundary region based on the separability of image features. A separability value is used which can be calculated by linear discriminant analysis.[9] A pixel with a separability value that is higher than the threshold value is detected as an edge. If we divide a local region into two small regions 1 and 2 with a central focus on a target pixel, the separability of a target pixel η is defined by

$$\eta = \frac{\sigma_b^2}{\sigma_T^2}, \tag{9}$$

$$\sigma_b^2 = n_1(\bar{P}_1 - \bar{P})^2 + n_2(\bar{P}_2 - \bar{P})^2, \tag{10}$$

$$\sigma_T^2 = \sum_{i=1}^{N} (P_i - \bar{P})^2, \tag{11}$$

where N is the number of pixels in the entire region, n_1 is the number of pixels in region 1, n_2 is the number of pixels in region 2, $\bar{P}_1$ is the average of the pixel values in region 1, $\bar{P}_2$ is the average of the pixel values in region 2, $\bar{P}$ is the average of the pixel values in the entire region, σ_T is the total variation, and σ_b is the variation between classes. This method uses a set of four masks for four directions (i.e., 0°, 45°, 90°, 135°). Here, the η value of each mask is calculated, and the highest value for η is adopted. This process is applied to all pixels, and pixels with a value higher than the threshold value are extracted as an edge. Thus, images are converted into edge images. This method has the advantages of being robust against noise and blurred edges. Therefore, it can detect edges for microscopy images with a great deal of noise. In addition, it can detect robustly under different shooting conditions because it is insulated from the influence of changing the threshold value.

Line Detection

RANSAC is used to calculate line equations for edge images. In our method, the target data are the pixels of edge images. Consider variables A, B, and C, which are defined by

$$Ax + By + C = 0. \tag{12}$$

The following equations were developed by applying the method of maximum likelihood estimation and the method of Lagrange multipliers:[10]

$$J = \frac{1}{2}\left(\begin{bmatrix} A \\ B \end{bmatrix}, \boldsymbol{M}\begin{bmatrix} A \\ B \end{bmatrix}\right), \tag{13}$$

$$\boldsymbol{M} = \begin{bmatrix} \sum_{a=1}^{N}(x_a - m_x)^2 & \sum_{a=1}^{N}(x_a - m_x)(y_a - m_y) \\ \sum_{a=1}^{N}(x_a - m_x)(y_a - m_y) & \sum_{a=1}^{N}(y_a - m_y)^2 \end{bmatrix}, \tag{14}$$

$$C = -Am_x - Bm_y, \tag{15}$$

where m is the coordinate of the center of mass of the target data and M is a coefficient matrix. Eqs. (13)–(15) are applied to data extracted with RANSAC to obtain conclusive parameters. In addition, RANSAC is applied again to data that have been eliminated but are in the range of the extraction line to detect multiple lines.

Matching Images

Images are matched in order to synthesize two images. First, the points of intersection of two lines as detected with RANSAC are calculated. Points with coordinates very far from the origin are removed. Next, all the triangles that can be generated from these points are created. That is, ${}_nC_3$ triangles are generated from n points of intersection; C is combination and n is the sum of intersection numbers. We combine three points among n points. Then, similar triangles in the image are eliminated. After this process is applied to two images, similar triangles between these images are matched. The ratio of the lengths of a triangle's sides is the ratio of the display magnification. The ratio of the display

DOI: 10.2352/ISSN.2470-1173.2016.14.IPMVA-372

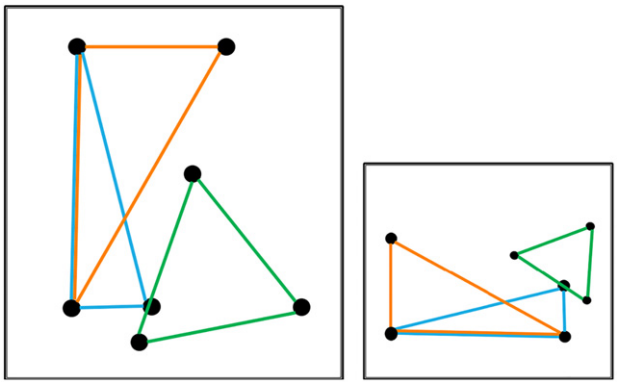

Figure 8. Schematic of matching triangles.

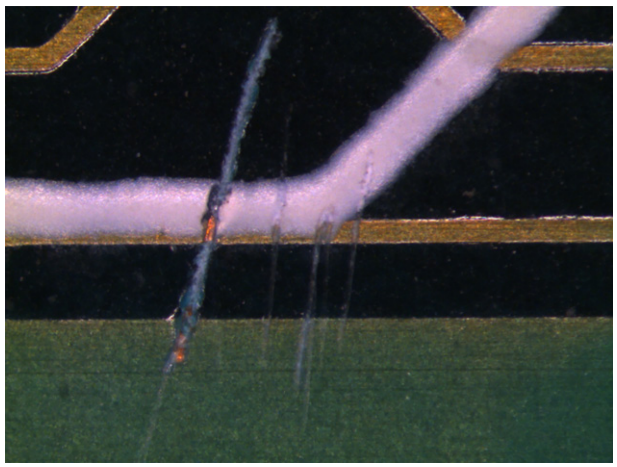

Figure 9. Low-resolution image.

magnification is estimated from all similar triangles. The most common magnification ratio is adopted for the data. Affine transformation is applied to match each coordinate of a triangle in two images. This provides image synthesis that is robust against rotation and scale transition. Figure 8 shows an example of matching images. The red triangle in the right figure is similar to the same color triangle in the left figure. In this figure, the ratio of the lengths of the red triangles is equal to the ratio of the lengths of the blue triangles, but the ratio of the lengths of the green triangles is different. Thus, the green triangles are regarded as a failure and are removed. Then, the images are transformed so that the coordinates of the other triangles correspond. This allows for stable synthesis.

Result of Image Synthesis Based on Edge Information

We applied the proposed method to images measured with different microscopes. Figure 9 shows an image that was captured at 2.5× magnification. Table I lists the shooting conditions. Figure 10 shows an image that was captured at 10× magnification. Table II lists the shooting conditions. The resolution in Fig. 9 is 1.98 μm, and the resolution of Fig. 10 is 0.22 μm. It was difficult for the method based on feature points to synthesize these images. We converted Fig. 10 to edge images. Figure 11 shows the edge image from using the proposed method and Figure 12 shows the edge

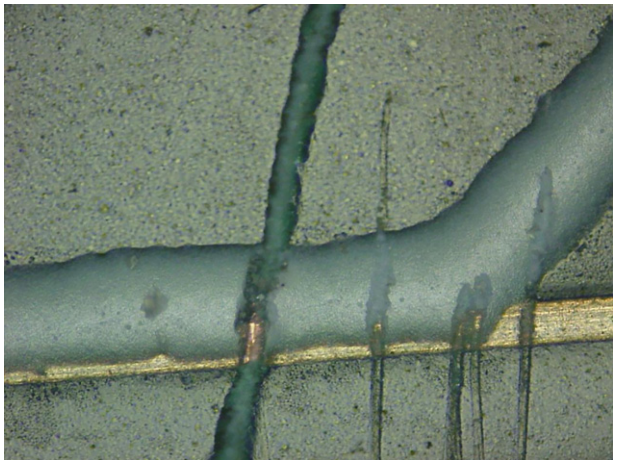

Figure 10. High-resolution image.

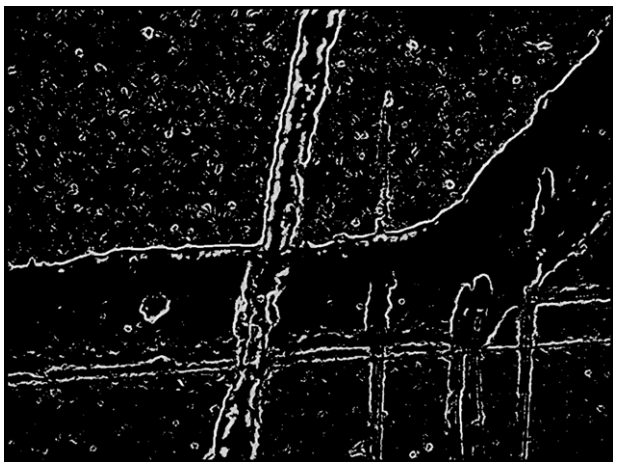

Figure 11. Edge image based on separability.

image from using the Canny edge. Our method resulted in less noise than that with the Canny edge. Moreover, our method detected edges precisely. With the Canny edge method, we needed to set thresholds carefully depending on the input image. In contrast, we were able to robustly apply the proposed method to images with different shooting conditions because it is insulated from the influence of varying thresholds. Next, we extracted lines from Fig. 11 with RANSAC, as shown in Figure 13. Figure 14 shows the results of using the proposed method on Figs. 9 and 10. Table III lists the calculation parameters. The processing time of our method was 47.356 [s]. We were able to match the scale magnification, position, and display angle of images with a resolution difference of 9×. Thus, we consider this method to be more effective than the method based on feature points for images captured under very different shooting conditions.

Evaluation of Our Methods

We proposed two image synthesis methods based on feature points and edge information. In this section, we evaluate the success rate of each method. If the rate of display magnification calculated by our method is within 10% of the true value, and the display angle and location of the each

DOI: 10.2352/ISSN.2470-1173.2016.14.IPMVA-372

Table II. Shooting conditions with a laser microscope.

Device name	Laser microscope VK-X100
Optical system	Confocal microscopy with pinhole
Light source	100 W halogen
Imaging device	1/3″ CCD image sensor
Sensor resolution	3072 × 2304

Table III. Calculation results.

	High-resolution image	Low-resolution image
Number of intersections	19	23
Number of triangles (before elimination)	683	1,185
Number of triangles (after elimination)	150	183
Target intersection coordinates	(374,607) (522,596) (365,773)	(193,284) (276,280) (189,378)
Estimated ratio of display magnification	0.5632	
Number of estimated counts	52	

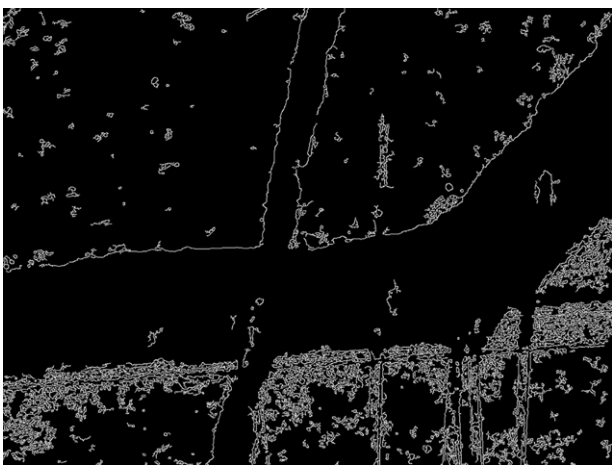

Figure 12. Edge image with Canny edge.

experimental result are roughly correct, we consider that the experiment is successful. We applied the method based on feature points to images obtained by two microscopes, which are shown in Tables I and II. Table IV summarizes the experimental results.

The method based on feature points has a high rate of success for images obtained with the same microscope. As described in the third section, we were able to synthesize images with different magnifications. In the case of using the same microscope, when measurement images are dark or have low brightness changes, it is difficult to detect

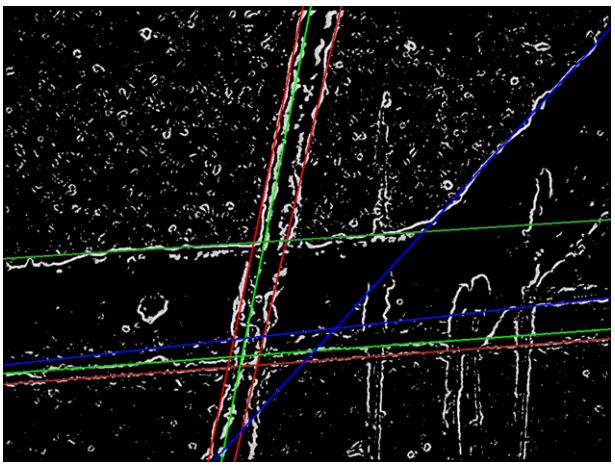

Figure 13. Results of line detection with RANSAC.

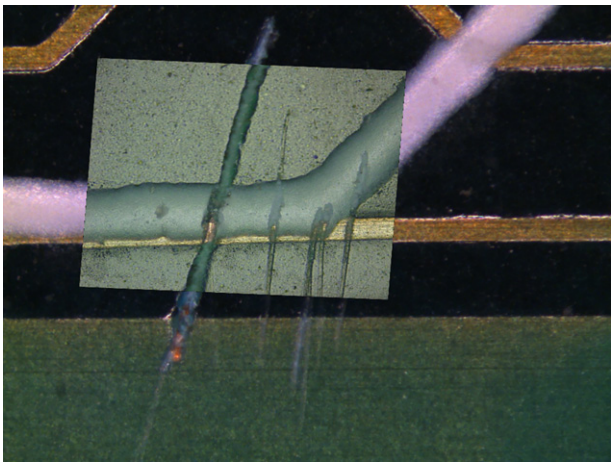

Figure 14. Results of image synthesis based on edge information.

feature points by SURF. Hence, we could not synthesize these images. However, we were able to synthesize 80% of images obtained with the same microscope. By contrast, when we used different microscopes, the rate of success was 4%. As described in the Outline of the Method Based on Edge Information section, if we take a picture of the same target under different conditions (e.g., different microscopes or sensors), it is difficult to synthesize these images by using the method based on feature points. Thus, we apply the method based on edge information to images obtained with different microscopes. Table V lists the results.

The rate of success was 32%, which is a little low. However, we made a significant improvement in the rate of success as compared with the method based on feature points. We can increase the success rate of synthesis of all images by selecting methods according to target images. When we applied the method based on feature points to images obtained with the same microscope and applied the method based on edge information to images with different microscopes, the success rate of synthesis of all images was 74.4%. We improved the success rate compared with the method only based on feature points. Figure 15 shows

DOI: 10.2352/ISSN.2470-1173.2016.14.IPMVA-372

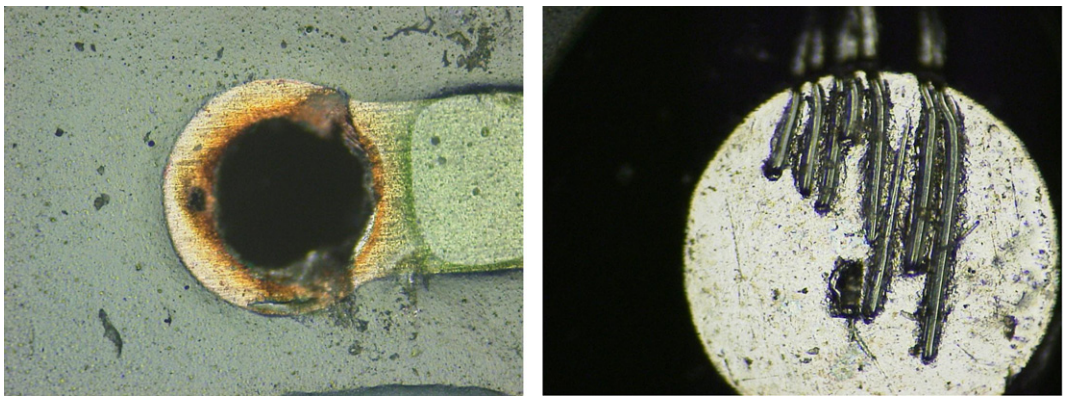

Figure 15. Examples of failure.

Table IV. Results of applying the method based on feature points.

	Images obtained with the same microscope	Images obtained with different microscopes	All images
Sample number [pair]	131	25	156
Success number [pair]	107	1	108
Rate of success [%]	81.7	4.0	69.2

Table V. Results of applying the method based on edge information.

	Images obtained with different microscopes
Sample number [pair]	25
Success number [pair]	8
Rate of success [%]	32.0

examples of failure of applying the method based on edge information to images obtained with different microscopes. We currently synthesize images with lines that are extracted by RANSAC. Since we cannot extract lines from images that have circle shapes, we are not able to synthesis these images. However, we can use ellipse equations to improve the RANSAC performance. If we obtain the parameters of the ellipse equation from images, we can synthesis images that have circle shapes using the parameters of the ellipse. We will probably increase the success rate of image synthesis by improving RANSAC.

GENERATION OF THE MULTI-RESOLUTION MODEL

Structure of the Multi-resolution Model

We not only synthesized images under different shooting conditions but also structured a multi-resolution model that a user can use to arbitrarily operate the display magnification and range. One related work in the CG field is multiscale texture synthesis.[11] This work proposed a multiscale setting for example-based texture synthesis, enabling the creation of textures spanning large or infinite ranges of scale. Based on this technique, we developed the multi-resolution model for images using microscopes at the nano- and micro-scale. In order to apply measurements, we need to simultaneously display the entire structure and fine details of an observed object. Moreover, we display images while maintaining the pixel resolution on each image. We developed a model that changes the displayed image depending on the user operation. Figure 16 shows the model. The red and blue rectangle areas are high-resolution images that have been synthesized, and the black dashed rectangles are display ranges. The model is a multi-layer construction. The user can shift the observation point arbitrarily. In addition, we apply mipmap, which is a general and well-researched method in the CG field[12] to our system. Mipmap generates image pyramids and improves the efficiency of the texture display. The model changes the displayed image by using mipmap depending on the magnification as needed. That is, it displays textures of higher-magnification images as the user increases the display magnification and narrows the range of view

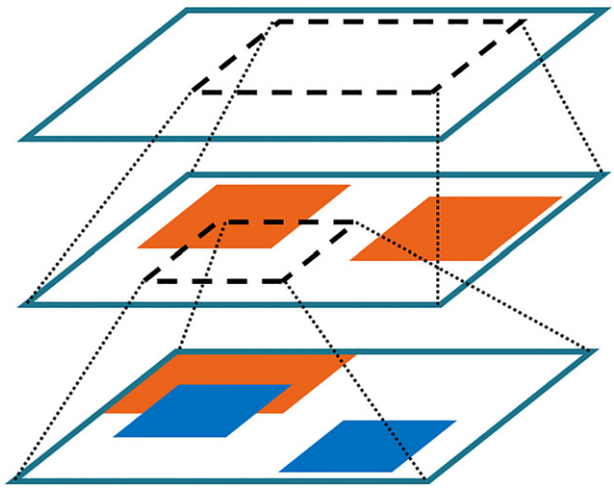

Figure 16. Multi-resolution model of images.

DOI: 10.2352/ISSN.2470-1173.2016.14.IPMVA-372

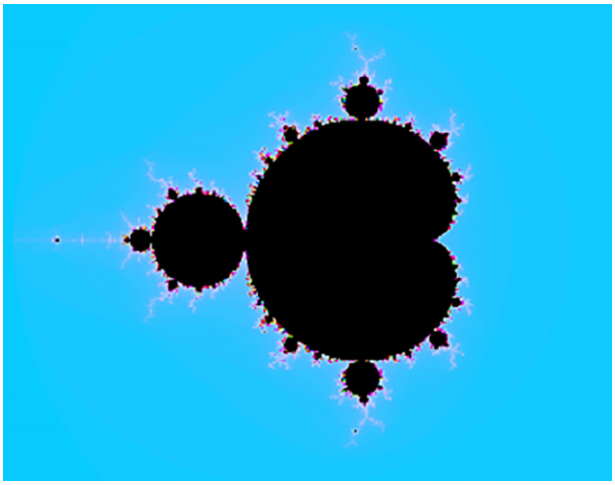

Figure 17. Overall view of the Mandelbrot set.

on a base image. Therefore, the user can get more precise information within a specified range.

We now present examples of applying the multi-resolution model to the Mandelbrot set. A figure with self-similarity is called a fractal. The Mandelbrot set is a fractal figure defined by

$$z_{n+1} = z_n^2 + C. \tag{16}$$

Figure 17 shows a Mandelbrot set generated with a program. In this program, the colors of the Mandelbrot set vary in parallel with the situation of convergence. In other words, the colors change depending on the reduction scale. We generated an image that shows part of Fig. 17 enlarged 100×, as shown in Figure 18. The left side of Fig. 18 is the generated image, and the right side is a zoomed-in image of the generated image. There should be more detailed similar figures around the original figures because the Mandelbrot set has self-similarity. However, we could not obtain more detailed information beyond the pixel resolution by zooming in the generated image because the images could not display more detail than the image resolution. Thus, we applied the multi-resolution model to images that were generated in the same range with different details. Figure 19 shows the result when we applied our model to images of the Mandelbrot set. The right side shows a zoomed image of the left side. The image resolution increases with each image border. Fig. 19 shows images with different resolutions, in contrast to Fig. 18. We could observe a wide range with different image resolutions. Thus, the multi-resolution model allows a user to arbitrarily vary the display range or image resolution. This model enables any user to obtain the entire structure and fine details of the observation object by displaying images of different resolutions at the same time.

Discussion of the Generated and Displayed Multi-Resolution Model

We were able to generate a multi-resolution model for images by using the method presented in the previous sections. We implemented a system where a user can arbitrarily change the display area and magnification of the base image with our model. Figure 20 shows the result when we applied our system to microscopy images with different magnifications. The left window shows an enlarged image of an area selected by the user. The user can arbitrarily vary the display area and magnification in this window. The textures of the high-resolution images displayed in this window change depending on the display magnification as needed. The right window shows the rectangle domain in the left window. The user can view the specified range with high resolution and obtain the entire structure of the observation object and positional relationship of each image. We implemented a system that can zoom and synthesize images while maintaining the pixel resolution of each image. Thus, high-resolution images are displayed while maintaining the pixels during zooming. Figure 21 shows the difference in pixel sizes. The left image shows part of the synthesized image, and the right image shows an enlarged version of the red rectangle area in the left image. This figure shows the borderline between the high-resolution and low-resolution images. It describes the size of one pixel in each region with white grid lines. The pixel of the high-resolution image is smaller than that of the low-resolution image. Therefore, our system can display the remaining detailed information. In this manner, we developed a multi-resolution model for images.

One conventional method creates and views high-resolution gigapixel images by capturing and coupling

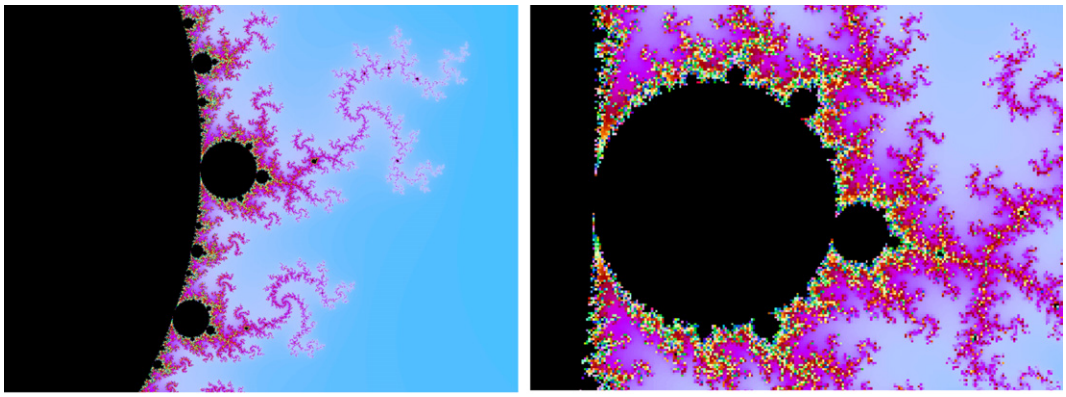

Figure 18. Part of the Mandelbrot set enlarged 100×.

DOI: 10.2352/ISSN.2470-1173.2016.14.IPMVA-372

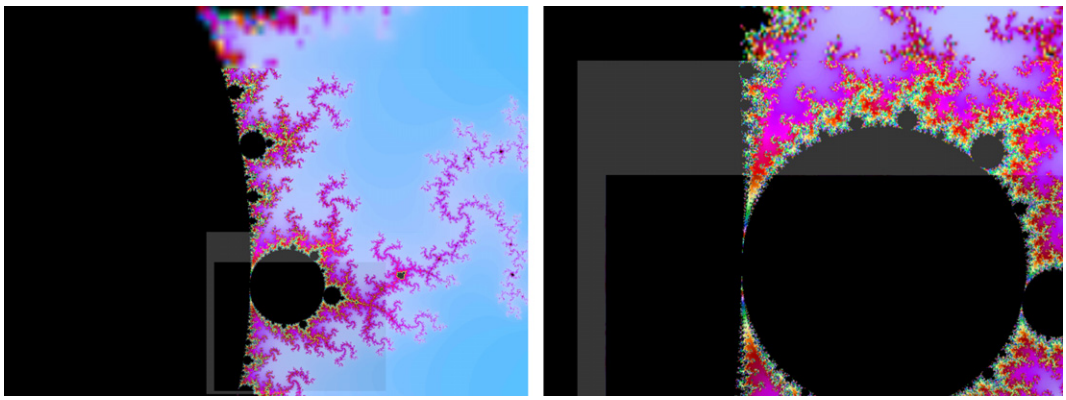

Figure 19. Result of applying our model to images of the Mandelbrot set.

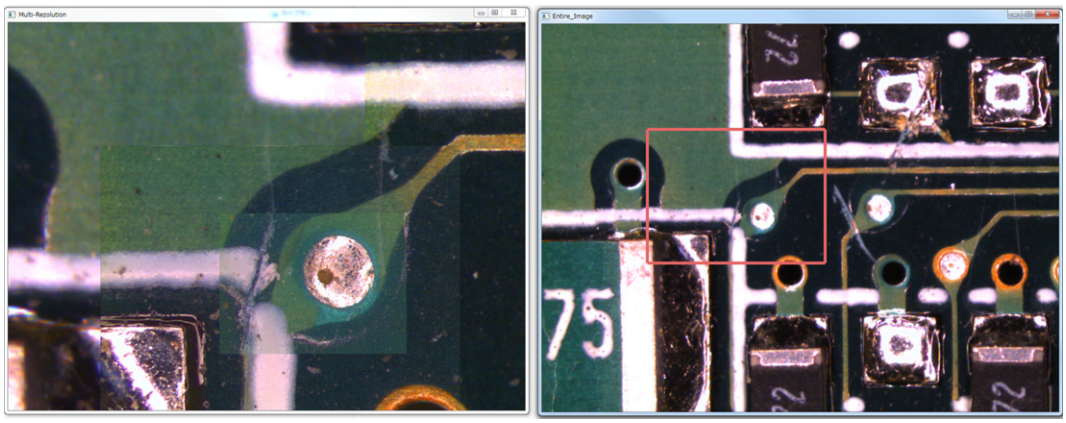

Figure 20. Result of the multi-resolution model.

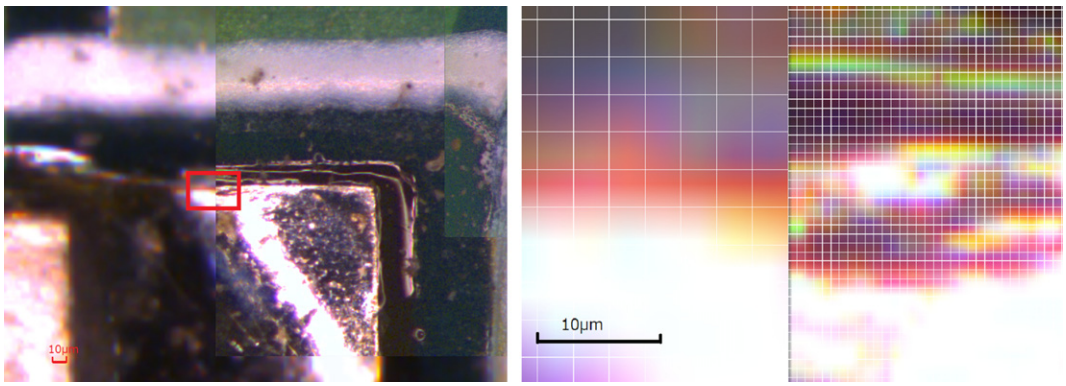

Figure 21. Pixel size of each resolution image.

images.[1] We compared our system with the conventional one. First, we compared the system structure between these systems. In the conventional method, the system displays a wide range of images with high resolution by coupling images that were captured by turning the camera angle. The targets of the system are continuous shooting images that were captured with a specific camera. Furthermore, when assembling images, the system uses information on shooting conditions. In contrast, in our system, high-resolution images are displayed on low-resolution images by synthesizing images taken under different conditions. The targets of our system are images taken under different conditions, and our system does not use the shooting conditions to synthesize images, such as the image magnification and the types of microscopes. Next, we compared processing times. In the conventional method, the processing time to generate a 4.5 gigapixel image is 270 min, that is, the processing time is 3.6 seconds per megapixels. In our system, the processing time of the method based on feature points is 0.82 seconds per megapixel and the processing time of the method based on edge information is 29 seconds per megapixel. The method based on feature points can process rapidly but the

DOI: 10.2352/ISSN.2470-1173.2016.14.IPMVA-372

method based on edge information needs a lot of time to process. Thus, we consider parallel processing on a GPU in order to speed up the method based on edge information.

CONCLUSION

In this article, we suggest two image synthesis methods based on feature points and edge information for microscopy images taken under different shooting conditions. We structured a multi-resolution model that can be used to arbitrarily vary the display area and magnification to obtain the entire structure and fine details of the observed object.

In future work, we will try to increase the success rate of image synthesis by improving RANSAC. Furthermore, we will apply iterative closest point (ICP)[13] to roughly match images for more precision. Moreover, we will utilize a technique of creating smooth visual pyramids from dissimilar imagery[14] to create a system that will generate an image with a magnification between those of the original images with different magnifications. Lastly, we will consider a method to generate a multi-resolution model in three dimensions.

ACKNOWLEDGMENTS

This work was supported by JSPS KAKENHI Grant-in-Aid for Challenging Exploratory Research, Grant Number 50254066. The authors also acknowledge the stimulated discussion in the meeting of the Cooperative Research Project of Research Institute of Electronics, Shizuoka University.

REFERENCES

[1] J. Kopf, M. Uyttendaele, O. Deussen, and M. F. Cohen, "Capturing and viewing gigapixel images," ACM Trans. Graph. **26**, 93 (2007).
[2] H. Bay, A. Ess, T. Tuytelaars, and L. V. Gool, "Speeded-Up Robust Features (SURF)," Comput. Vis. Image Underst. **110**, 346–359 (2008).
[3] H. Fujiyoshi and M. Mitsuru, "Gradient-based image local features," J. Japan Soc. Precis. Eng. **77**, 1109–1116 (2011).
[4] M. A. Fischler and R. C. Bolles, "Random sample consensus: a paradigm for model fitting with applications to image analysis and automated cartography," Commun. ACM **24**, 381–395 (1981).
[5] P. Perez, M. Gangnet, and A. Blake, "Poisson image editing," ACM Trans. Graph. (SIGGRAPH 2003) **22**, 313–318 (2003).
[6] N. Kawai, T. Sato, and N. Yokoya, "Image inpainting considering brightness change and spatial locality of textures and its evaluation," Adv. Image Video Technol. **5414**, 271–282 (2009).
[7] K. Fukui, "Edge extraction method based on separability of image features," IEICE Trans. Inf. Syst. **E78-D**, 1433–1538 (1995).
[8] K. Fukui, "Contour extraction method based on separability of image features," IEICE Trans. Inf. Syst. **J80-D-2**, 1406–1414 (1997).
[9] N. Otsu, "A threshold selection method from gray-level histograms," Trans. Syst. Man Cybern. **9**, 62 (1979).
[10] Y. Sugaya and K. Kanaya, "Optimization computation for 3-D understanding of images [1]: Line fitting," J. IEEE **92**, 229–233 (2009).
[11] C. Han, E. Risser, R. Ramamoorthi, and E. Grinspun, "Multiscale texture synthesis," ACM Trans. Graph. **27**, Article 51 (2008).
[12] Tevs Art, Ivo Ihrke, and Hans-Peter Seidel, "Maximum mipmaps for fast, accurate, and scalable dynamic height field rendering," *Proc. 2008 Symposium on Interactive 3D Graphics and Games* (ACM, 2008).
[13] Paul J. Besl and Neil D. McKay, "A method for registration of 3-D shapes," IEEE Trans. Pattern Anal. Mach. Intell. **14**, 239–256 (1992).
[14] C. Han and H. Hoppe, "Optimizing continuity in multiscale imagery," ACM Trans. Graph. **29**, 171 (2010).
[15] W. Huamin, J. O'Brien, and R. Ramamoorthi, "Multi-resolution isotropic strain limiting," ACM Trans. Graph. **29** (2010).